Published in final edited form as:
*Neuroimage*. 2012 February 1; 59(3): 2860–2870. doi:10.1016/j.neuroimage.2011.09.049.

# "Roles for the pre-supplementary motor area and the right inferior frontal gyrus in stopping action: electrophysiological responses and functional and structural connectivity"

**Nicole C Swann**[1], **Weidong Cai**[2], **Christopher R Conner**[3], **Thomas A Pieters**[3], **Michael P Claffey**[2], **Jobi S George**[2], **Adam R Aron**[2], and **Nitin Tandon**[3,*]

[1]Department of Neuroscience University of California San Diego

[2]Department of Psychology, University of California San Diego

[3]Department of Neurosurgery, University of Texas Medical School at Houston

## Abstract

Both the pre-supplementary motor area (preSMA) and the right inferior frontal gyrus (rIFG) are important for stopping action outright. These regions are also engaged when preparing to stop. We aimed to elucidate the roles of these regions by harnessing the high spatio-temporal resolution of electrocorticography (ECoG), and by using a task that engages both preparing to stop and stopping outright. First, we validated the task using fMRI in 16 healthy control participants to confirm that both the preSMA and the rIFG were active. Next, we studied a rare patient with intracranial grid coverage of both these regions, using macrostimulation, diffusion tractography, cortico-cortical evoked potentials (CCEPs) and task-based ECoG. Macrostimulation of the preSMA induced behavioral motor arrest. Diffusion tractography revealed a structural connection between the preSMA and rIFG. CCEP analysis showed that stimulation of the preSMA evoked strong potentials within 30 ms in rIFG. During the task, when preparing to stop, there was increased high gamma amplitude (~70–250 Hz) in both regions, with preSMA preceding rIFG by ~750 ms. For outright stopping there was also a high gamma amplitude increase in both regions, again with preSMA preceding rIFG. Further, at the time of stopping, there was an increase in beta band activity (~16 Hz) in both regions, with significantly stronger long-range coherence for successful vs. unsuccessful stop trials. The results complement earlier reports of a structural/functional action control network between the preSMA and rIFG. They go further by revealing between-region timing differences in the high gamma band when preparing to stop and stopping outright. They also reveal strong between-region coherence in the beta band when stopping is successful. Implications for theories of action control are discussed.

### Keywords

Electrocorticography; functional MRI; stop signal task; beta frequency band; gamma frequency band; cognitive control; inhibitory control



[*]Corresponding author: Nitin Tandon Dept of Neurosurgery University of Texas Medical School at Houston Nitin.Tandon@uth.tmc.edu.

## INTRODUCTION

Lesion studies and Transcranial Magnetic Stimulation show that stopping an initiated response depends on the integrity of the right inferior frontal gyrus (rIFG) as well as the presupplementary motor area (preSMA) (reviewed by Aron, 2010; Chambers et al., 2009; Chikazoe, 2010; Levy and Wagner, 2011; Nachev et al., 2008). Additionally, diffusion tensor imaging (DTI) tractography shows that the IFG and the preSMA are structurally connected to one another, and to the basal ganglia, comprising a putative network for action control (Aron et al., 2007; Ford et al., 2010; Forstmann et al., 2010; Johansen-Berg et al., 2004). Electrophysiological studies have begun to characterize the neural communication within this putative network, pointing to increased activity in the beta frequency band during successful stopping (Kühn et al., 2004; Marco-Pallares et al., 2008; Swann et al., 2011; Swann et al., 2009).

Yet, while the preSMA and the rIFG are key nodes of this putative network, their relative functional roles in stopping are still unclear. For instance, it has been suggested that they could both be important for inhibitory control, or one could be important in monitoring for the stop signal and/or detecting conflict and another for implementing inhibitory control (Duann et al., 2009; Hampshire et al., 2010; Mostofsky and Simmonds, 2008; Sharp et al., 2010; Verbruggen et al., 2010). Notably, recent fMRI studies show that both regions are active when preparing to stop, as well as during outright stopping (Chikazoe et al., 2009b; Jahfari et al., 2009; Vink et al., 2005; Zandbelt and Vink, 2010). This raises the additional possibility that one or both regions are involved in setting up the stopping network in advance so that inhibitory control can subsequently be triggered when the stop signal is detected. While we refer to this as `preparing to stop' we note that it could also be described as increased response caution, favoring accuracy over speed, or proactive inhibitory control. If the preSMA is important for setting up the stopping network, i.e. a task configuration role (Rushworth et al., 2004) then it should be active soon after a cue that instructs the participant that stopping is likely, and before the rIFG; whereas if the rIFG is important for this function then the reverse timing relation should be observed. Testing this with fMRI is difficult because of the poor temporal resolution. Instead, we studied a single, rare, patient who had electrocorticography (ECoG) electrodes implanted over both the preSMA and the rIFG.

We designed a new task to engage both preparing to stop and outright stopping (Figure 1). Each trial began with a cue “Maybe Stop” or “No Stop” which was followed by a Go stimulus and then, on Maybe Stop trials alone, this was sometimes followed by a stop signal. By comparing Maybe Stop and No Stop trials we could examine the preparing-to-stop process; while by comparing Maybe Stop successful stop vs. unsuccessful stop trials (or Maybe Stop successful stop compared to Maybe Stop go trials or baseline) we could examine outright stopping. We used fMRI in healthy young participants to confirm that this task activated the preSMA and rIFG as expected.

In the patient we performed macrostimulation and DTI, and we collected cortico-cortical evoked potentials (CCEP) and task-related ECoG. First, macrostimulation was applied systematically to different electrode contacts in dorsal-medial frontal cortex while the patient performed vocal or manual movements. We aimed to confirm prior reports that macrostimulation of anterior SMA (preSMA) induces motor arrest (Fried et al., 1991; Luders et al., 1988). Second, DTI was used to verify the connection between the preSMA and the rIFG that has been established in normative populations (Aron et al., 2007; Ford et al., 2010; Forstmann et al., 2010; Johansen-Berg et al., 2004). Third, we evaluated task-independent functional connectivity between the preSMA and the rIFG using CCEPs (Matsumoto et al., 2007; Matsumoto et al., 2004). By stimulating different dorsomedial

contacts (in a pair-wise fashion) we could `map' the spatial and temporal responses in the right lateral frontal cortex. We were interested in determining whether CCEPs from specific preSMA electrodes elicited short-latency responses within specific rIFG electrodes. Finally, we recorded ECoG while the patient performed the Maybe Stop/No Stop task.

For preparing to stop (time-locked to the cue) we anticipated high gamma amplitude changes in both rIFG and preSMA since fMRI studies of preparing-to-stop have shown BOLD signal increases in both these regions (Chikazoe et al., 2009b; Jahfari et al., 2009; Vink et al., 2005; Zandbelt and Vink, 2010), and high gamma increases are associated with the BOLD signal (Conner et al., 2011; Logothetis et al., 2001; Scheeringa et al., 2011). Our observations go beyond previous reports by identifying *when* these regions are involved in preparing to stop, which could help differentiate their roles.

For outright stopping (time-locked to the stop signal) we aimed to examine both high gamma and beta band activity. High gamma activity was anticipated in both regions since they show BOLD signal increases for stopping, and, as described earlier, high gamma increases are associated with the BOLD signal (Conner et al., 2011; Logothetis et al., 2001; Scheeringa et al., 2011). We also expected an increase in beta band amplitude over rIFG for successful vs. unsuccessful stop trials based on our earlier report (Swann et al., 2009). We also predicted that there would be beta band increases in the preSMA, given the evidence for involvement of this region in response control and its structural connectivity to rIFG. Further, we planned to examine beta band coherence between the preSMA and the rIFG. Coherence is a measure of functional connectivity thought to reflect communication between brain areas (Fries, 2005). If beta band coherence between the preSMA and the rIFG is important for successful stopping then it should be stronger on successful than unsuccessful stop trials.

## METHODS

### Experiment 1: fMRI in healthy adults

**Participants—**Sixteen young adults (8 female, 18–28 years old) were recruited from the local community. All participants provided written consent in accordance with the Internal Review Board of the University of California at San Diego. They received monetary compensation.

**Task—**An event-related Maybe Stop (MS) / No Stop (NS) task was used (see Figure 1A). On each trial, a cue was presented in the center of the screen for 1 sec. The cue was either the words “Maybe Stop” (red on a black background) or “No Stop” (green on a black background) equiprobably. A go signal (white arrow) followed the cue. Participants made right index or left index finger presses in response to rightward and leftward pointing arrows as quickly as possible. In the MS condition, a beep (stop signal) followed the go signal, on 50% of trials, with a variable delay. Participants were instructed to withhold responses when the stop signal occurred. In order to achieve 50% stopping accuracy, the stop signal delay was dynamically changed based on behavior (for full details of the procedure see Aron and Poldrack, 2006). The initial stop signal delay was 150 ms. The response window was 1 second and the inter-trial-interval was jittered between 1.5–5 seconds. Five participants performed two blocks of the task and 10 participants performed one block of the task (because of limited scanning time). Each block included 20 MS_Go trials, 20 MS_Stop trials and 40 NS_Go trials. Participants were practiced on the task initially before entering the scanner and were encouraged to respond quickly on go trials and to do their best to stop their response on stop trials.

**MRI data collection—**MRI data were acquired with a 3T GE SIGNA HDX scanner with an eight channel head coil at the UCSD Center for functional MRI. A high-resolution T1 3D FSPGR scan was acquired for the purpose of registration (slice thickness, 1 mm; TR, 7.8 seconds; TE, 3 seconds; matrix, 192 × 192; FOV, 256; 172 sagittal slices, voxel size 1.3 × 1.3 × 1 $mm^3$). Each functional scan comprised 180 T2*-weighted echo planar images (slice thickness, 4 mm; TR, 2 seconds; TE, 30 ms; flip angle, 90°; matrix, 64×64; FOV, 200; 32 axial slices, voxel size 3.1 × 3.1 × 4 $mm^3$).

**Behavioral Analysis—**We calculated mean RT and accuracy for each of MS_Go and NS_Go trials; the average stop signal delay (after staircase convergence); and stop signal reaction time (SSRT) (for details see Aron and Poldrack, 2006).

**Functional MRI data preprocessing and analysis—**MRI data were processed using the FSL software library (www.fmrib.ox.ac.uk/fsl). The functional series were aligned to compensate for small head movements. A two-step registration procedure was applied whereby the EPI images were first registered to the participant's own T1 image, then normalized to the MNI152 template using 12-parameter affine registration. All data were spatially smoothed with a Gaussian kernel of 5 mm at full-width half-maximum and were high-pass filtered at 66 s.

Five regressors were defined for each scan for each participant: NS_Go (correct NS go trials), MS_Go (correct MS go trials), MS_SS (MS successful stop trials), MS_US (MS unsuccessful stop trials), and Others (i.e. incorrect go trials or omissions on go trials). The regressors were modeled at the onset of the Go stimulus, and they were convolved with a canonical hemodynamic response function. For each participant and each scan, we generated the two main contrasts of interest: i.e. MS_Go vs. NS_Go (preparing to stop) and, i.e. MS_SS vs. MS_Go (outright stopping).

Functional MRI data processing was carried out using FEAT (FMRI Expert Analysis Tool) version 5.98. Higher-level analysis was performed by first doing fixed-effects across scans for each participant (for the participants who had two scans), followed by a random-effects analysis across all participants for each of the two contrasts. Higher-level analysis was carried out using FLAME (FMRIB's Local Analysis of Mixed Effects) stage 1 (Beckmann et al., 2003; Woolrich, 2008; Woolrich et al., 2004). Activations were corrected for multiple comparisons at $z>2.3$, $p<0.05$ whole-brain cluster corrected.

## Experiment 2: Case study

**Participant—**The participant was a 27 year old, right-handed, male undergoing evaluation for possible resective surgery to treat medically intractable epilepsy. He was enrolled into the study after providing informed consent according to a protocol at the University of Texas at Houston Medical School's committee for protection of human participants. We note that the locus of his epileptic activity was subsequently determined to not include either the preSMA or the IFG. Besides the epilepsy, this patient was judged to be neurologically normal. Formal neuropsychological testing revealed a verbal IQ of 106 and a performance IQ of 118.

**Subdural electrode placement and localization—**The electrode localization methodology and recording strategies used were similar to those previously described (Khursheed et al., 2011; Swann et al., 2009; Tertel et al., 2010). Briefly, subdural electrodes spaced 1 cm apart were implanted (Tandon, 2008). A post-operative CT scan was co-registered with pre-implantation MRI. Subdural electrodes were localized on the CT scan, projected onto a cortical surface model generated in FreeSurfer (Dale et al., 1999), and

visualized with SUMA software as spheres (Saad et al., 2003). These locations were verified using intra-operative photographs. Electrodes were then given anatomical labels, in semi-automated fashion, using a FreeSurfer parcellation scheme.

**Macrostimulation procedure—**Macrostimulation was carried out to localize functional zones prior to resection for epilepsy. A balanced faradic current was delivered at 50 Hz using a S88 Grass stimulator that generates trains of biphasic rectangular waves (Grass technologies, West Warwick, Rhode Island). The duration of each wave was 500 μs, and these were delivered in trains of 3–5 second duration via two contacts located on the cortical surface during performance of simple motor or verbal tasks described below. Current strength ranged from 1 – 10 mA, determined by overt phenomenology or the induction of after discharges in the concurrent ECoG (Tandon, 2008). To assess the impact on motor function, the patient was asked to open and close his hands rapidly (as if making a symbol for a flashing light) and articulation was assessed by asking him to recite the letters of the alphabet and to read from a card held about 20 inches in front of him.

**DTI acquisition and analysis—**DTI was acquired on a 3T whole-body MR scanner (Philips Medical Systems, Bothell WA) equipped with an eight channel SENSE head coil. One B0 (non-diffusion weighted) image volume and diffusion weighted images were collected with the Philips 32-directions diffusion encoding scheme (high angular resolution) with the “gradient overplus” option. Seventy axial slices were acquired with 1.75 mm pixels, 2 mm slice thickness, and a maximum b-value of 800 s/mm$^2$. Individual diffusion-weighted images volumes were realigned to the participant's skull-stripped anatomical MRI, and a single-model diffusion tensor was computed. Deterministic fiber tracking was performed with DTIQuery using the streamline tracking algorithm (STT) with optimal parameters (Akers et al., 2005; Sherbondy et al., 2005): path step size (in millimeters)=1.0, seed point spacing (in millimeters)=2.0, FA termination threshold=0.15, angle termination threshold (in degrees)=45, min pathway length (in millimeters)=5.0, and max pathway length (in millimeters)=300.0, and Euler's Method for STT numerical integration. We placed 1 cm wide cuboids (with minimal overlap) over each of the dorsomedial electrodes as seeds for the deterministic generation of tracts to remote regions. All connections to the opposite hemisphere were eliminated.

**CCEP acquisition and analysis—**Adjoining electrode pairs in the inter-hemispheric electrode array were stimulated in bipolar fashion using single pulses (10 mA, 500 μs, 1 Hz for 50 seconds – total of 50 pulses for each pair), delivered by a Grass Stimulator. Concurrent ECoG was performed at 1000 Hz. All channels were referenced to an average of all intracranial electrodes except the stimulating electrodes, and electrodes within 2 cm from the site of stimulation, which served to eliminate effects of the stimulation artifact. The 50 epochs were time-locked, averaged and displayed as traces of the mean +/− 3 SEM. These tracings were compared to a baseline artifact-free ECoG trace (>60 sec long) acquired separately during the same recording session with the patient awake and at rest. Channels with significant ($p<0.001$) shifts from baseline with a maximum peak >150mV were identified for subsequent analysis using a t-test. We only included responses of latency >10 ms (to exclude stimulus artifact) and <30 ms (to eliminate indirect connections), and with amplitude <200 mV (to exclude direct current spread). The peak amplitude and time to peak for the CCEPs were computed for each recording channel. To depict the CCEPs graphically, spheroids whose size and color were dependent on the amplitude and latency of the CCEP, were generated and overlaid onto the cortical surface.

**ECoG paradigm, data acquisition and analysis—**The patient performed the MS/NS task described in Experiment 1 with four differences. First, the response window was

slightly longer: 1.5 seconds instead of 1 second to allow for slower responses from the patient if necessary. Second, the inter-trial interval was randomly varied from 1 to 1.4 second (in intervals of 100 ms) (instead of the longer ITI necessary for fMRI). Third, the patient was asked to respond using his left hand (index or middle finger), so we could sample ECoG from right primary motor cortex. (Note that this change is unlikely to change the results related to the stopping network since its right-laterality seems to be independent of hand used (Chambers et al., 2006; Konishi et al., 1998; Swann et al., 2009).) Fourth, the patient completed 7 blocks (96 trials each) of the task (since more trials are necessary for ECoG compared to fMRI).

Data were collected using an EEG 1100 Neurofax clinical Nihon Koden acquisition system recorded at 1000 Hz sampling rate. Trial onsets for the behavioral task were sent to the ECoG data acquisition computer via transistor–transistor logic pulses. Behavioral responses were recorded via button responses made with the patient's left hand, on a keyboard. All data were digitally re-referenced to a common average. This excluded channels with artifact or frequent ictal activity.

The ECoG analysis was nearly identical to our previous report (Swann et al., 2009). In brief, the data were filtered into 128 frequencies ranging from 2.5 to 250 Hz using a Gabor wavelet procedure. The filtered data were then epoched according to events of interest and averaged across trials. Analysis was time-locked to either the MS/NS cue or the stop signal. Note that for the MS/NS go comparison, the NS_Go trials were twice as frequent as MS_Go, so we randomly sub-sampled NS_Go trials to balance trial numbers. Omitting this step did not change the results. A baseline correction with a baseline period of 500 ms in the middle of the inter-trial interval was applied. Finally, the analytic amplitude for conditions relative to baseline were converted to z-scores using a permutation-based method with event indices randomly offset. To calculate z-scores for between condition comparisons (i.e. MS_Go compared to NS_Go or MS_SS to MS_US), a permutation-based, label-swapping, method was used. Where indicated, a “false discovery rate” (FDR) correction was applied to correct for multiple comparisons. For a given electrode, values for all time-points, frequencies, and conditions were considered for calculation of the FDR-corrected threshold. For further details see previous reports (Canolty et al., 2007; Swann et al., 2009).

In addition, because of previous research highlighting low frequency activity and its potential role in the network properties of these regions during stopping (Fries, 2005; Kühn et al., 2004; Swann et al., 2011; Swann et al., 2009), an additional analysis was conducted to closely examine low-frequency amplitude changes for rIFG and preSMA, as well as low-frequency coherence between these two regions for stop trials (time-locked to the stop signal). The amplitude changes were calculated in the same manner as described above except here with a prestimulus baseline of −500 to 0 ms relative to the stop signal, to more clearly visualize the instantaneous, task-related amplitude changes. Coherence is a measure of event-related amplitude and phase, which is thought to reflect functional connectivity, especially at low frequencies (Fries, 2005). It was computed using the corresponding auto-spectra and cross-spectra and ensemble averaging across trials as shown below.

$$Coh(t,f)=\frac{|W_{xy}(t,f)|}{\sqrt{W_{xx}(t,f)}\sqrt{W_{yy}(t,f)}} \text{ where } W_{xy}(t,f)=\frac{1}{N}\sum_{k=1}^{N}W_x(t,f).W_y*(t,f)$$

Here x and y refer to data from 2 channels. N is the number of trials and $W_x(t,f)$ is the complex analytic signal (dependant on time ($t$) and frequency ($f$)) obtained from filtering. Significance was calculated using procedures analogous to the event-related amplitude differences. For conditions relative to baseline z-scores were derived from a distribution

created using 10000 iterations of mean coherence values time-locked to random events. Between conditions (MS_SS vs MS_US) z-scores were calculated using a permutation method where a distribution of differences was created using the label swapping procedure.

# RESULTS

## Experiment 1: fMRI study in healthy adults

**Behavioral data—**RT for MS_Go trials was 533 ms and for NS_Go trials was 404 ms and this was a significant difference, $t(15)=5.86$, $p<0.001$, Table 1. This shows that participants were using the MS cue to prepare to stop (c.f.Chikazoe et al., 2009b; Jahfari et al., 2009). SSRT was estimated at 182 ± 50 ms. However, because of limited stop trials for some subjects (who only performed one block of the task), SSD values did not always have time to dynamically adjust to a 50% probability of stopping. Thus SSRT may not have been estimated very accurately for some subjects.

### Functional MRI

**Preparing to stop:** The contrast of MS_Go vs. NS_Go revealed significant activation of the preSMA and the rIFG, as well as other regions of prefrontal cortex and the parietal and temporal lobe in both hemispheres ($z>2.3$, $p<0.05$ whole-brain corrected, see Figure 1B, see Supplementary Table 1 for full details). Because reaction times differed for these two conditions the effect of RT variance on the brain activation was also examined by including an additional regressor of RT. Significant activations in the preSMA and the rIFG in the contrast of MS_Go versus NS_Go were still observed ($z>2.3$, $p<0.05$, cluster corrected*).* These results are similar to other studies using tasks that examine preparing to stop (Chikazoe et al., 2009b; Jahfari et al., 2009; Vink et al., 2005; Zandbelt and Vink, 2010). No significant activation was found for the contrast of NS_Go vs. MS_Go.

**Outright Stopping:** The contrast of MS_SS vs. MS_Go revealed significant activation of a predominantly right hemisphere network including the rIFG, parietal cortex, auditory cortex and other regions ($z>2.3$, $p<0.05$ whole-brain corrected, see Figure 1C and Supplementary Table 2 for full details). The activation pattern was consistent with prior studies of standard stop signal and Go/NoGo tasks (Aron et al., 2007; Aron and Poldrack, 2006; Cai and Leung, 2009; Chevrier et al., 2007; Garavan et al., 1999; Kenner et al., 2010; Konishi et al., 1998; Leung and Cai, 2007; Rubia et al., 2003; Xue et al., 2008). However, whereas those studies showed preSMA activation during outright stopping, here it was not detected, even when using a small volume correction for the anatomically defined preSMA region, and even with a lower threshold ($z=1.6$). A difference between the current task and those studies was that here outright stopping occurred in the context of preparing to stop. However, another study that examined preparing to stop, did show preSMA activation for outright stopping (Chikazoe et al. 2009). In that study, though, there was a 25% chance of a stop signal given a cue that stopping may occur, whereas here the probability was 50%. Thus, participants might have been in a greater state of stopping readiness in this paradigm, even on MS_Go trials, which could reduce the MS_SS vs. MS_Go difference, at least for preSMA. Another possibility is that we may have been under-powered, perhaps due to low-trial numbers, to see preSMA activation, especially if it is a subtle effect. Regardless, the current results establish for this particular behavioral paradigm that both the preSMA and the rIFG are activated when preparing to stop, and, that consistent with prior studies, the rIFG is activated for stopping outright.

## Experiment 2: Case study

**Behavior—**Mean RT was 618 ms for MS_Go trials and 491 ms for NS_Go trials and this was a significant difference, $t(334) = 6.38$, $p<.001$, Table 1. The average SSD was 379 ms

and SSRT was 239 ms. These values are comparable with the healthy adults in Experiment 1 and indicate that the patient performed the task well.

**Macrostimulation results—**Macrostimulation was carried out for all the dorsomedial frontal electrodes (entire inter-hemispheric grid, IH 1–20, see Figure 2) in a pair-wise bipolar fashion (e.g. inter-hemispheric electrodes (IH) 11 and 12). We found that stimulation at electrodes IH 1, 2, 3, 11, and 12 produced `motor arrest' (Table 2). Electrodes 11 and 12 in particular were the only pair to show a *bilateral* cessation of movement. These findings are consistent with previous macrostimulation studies that identified the anterior SMA along with the rIFG as “negative motor regions” (Fried et al., 1991; Luders et al., 1988). Given that stimulation at contacts 3,4 and 12,13 led to other effects, the electrodes that can be most clearly characterized as belonging to the pre-SMA were electrodes IH 1,2, and 11, with IH11 showing the most complete (bilateral) response characteristic of the anterior SMA/ preSMA region (Fried et al., 1991; Luders et al., 1988). All of these electrodes were within the posterior preSMA, as localized by FreeSurfer parcellation (see Figure 2 for locations) (Picard and Strick, 2003). Therefore, we focus on electrode IH11 for further analyses (talaraich coordinates: 0, 12, 51, see Supplementary Figure 1).

**DTI—**Deterministic tractography using cuboid seeds placed on electrode locations corresponding to the pre-SMA (i.e. IH 1, 2 and 11, 12) (Picard and Strick, 2003), revealed independent projections from the preSMA to the lateral prefrontal cortex, the midbrain, the medial prefrontal cortex and the medial parietal lobe. Strikingly, the connection to the lateral prefrontal cortex was specifically to the IFG. Moreover, the electrodes that corresponded to this connection most closely were IH11 (IH = inter-hemispheric) and LF16/15 (LF = lateral frontal) (Figure 3A and see Supplementary Table 3 for additional tract information and Supplementary Figure 2 for additional electrode locations). Although a white matter connection between the preSMA and the rIFG has previously been revealed by probabilistic tractography (Aron et al., 2007; Ford et al., 2010; Forstmann et al., 2010; Johansen-Berg et al., 2004) the current finding provides greater spatial specificity, and links structure and function in the same patient. Electrode IH11 was a contact at which macrostimulation induced motor arrest, and, as we show below, LF16 is the IFG electrode with both the clearest evoked potentials (when IH11 is stimulated) and the strongest ECoG responses during task performance.

**CCEPs—**Low frequency stimulation of the inter-hemispheric electrodes (IH 1–20) was carried out with concurrent high frequency sampling (1000 Hz) of the entire intracranial array to examine the (functional) electro-physiologic projections from preSMA. We were particularly interested in the connections to the lateral frontal cortex. To identify `direct' connections, we restricted ourselves to evoked changes occurring within the first 30 ms (Matsumoto et al., 2007; Matsumoto et al., 2004). These direct CCEPs were found to occur in the immediate neighborhood of the stimulating electrodes (presumably mediated by U fibers) but also remotely, in the lateral frontal lobe. The frontal lobe responses were centered in the posterior inferior frontal gyrus (LF 9, 10, 15, 16), in the lateral premotor cortex (LF 3) and in the middle frontal gyrus (LF1) (See Figure 3B and Supplementary Figure 3 for an example CCEP trace). No other brain regions showed such large, rapid responses (i.e. greater than 100 mV, within 30 ms). (For full details on the CCEP values for all channels, including those outside the lateral frontal regions, see Supplementary Table 3 and Supplementary Figure 2 for additional electrode locations). These findings provide functional connectivity evidence to corroborate the structural connection between the preSMA and the IFG. Importantly, the locations of the CCEPs in the lateral frontal cortex were remarkably spatially specific and corresponded well with the tract termination in rIFG

revealed by the DTI (i.e. LF16/15 see above) and with the ECoG results during task performance (LF16 see below).

**ECoG—**In Supplementary Figures 4–7 we show results from all electrodes in the anatomically defined preSMA and rIFG regions, however, in light of the above DTI and CCEP results, here we focus specifically on IH11 (preSMA) and LF16 (rIFG).

**Preparing to stop: preSMA and rIFG:** For the preSMA, time-locked to the MS or NS cue, there was an increase in high gamma band activity for both MS and NS trials (~70–250 Hz) relative to baseline (the inter-trial interval) (Figure 4). This increase began (defined as the point where the high gamma power first became significantly greater than baseline) after the MS or NS cue and approximately 500 ms before the Go stimulus (arrow) was presented ($p<0.05$ FDR corrected). The high gamma amplitude increase was much larger for MS_Go than NS_Go ($p<0.05$ FDR corrected), although this difference did not reach significance until after the Go stimulus.

For the rIFG, time-locked to the MS or NS cue, there was again an increase in high gamma band activity for each trial type. However, the above-baseline increase began about 250 ms after the Go cue, and the MS-NS difference did not emerge until about 500 ms later, around the time of movement onset ($p<0.05$ FDR corrected).

Thus, there was an increase in high gamma amplitude, more so for MS_Go than NS_Go trials, in both the preSMA and the rIFG, with the preSMA response began between the cue and the go stimulus and *preceding* the rIFG response. We note that high gamma band activity likely indicates local neuronal activity in each region (Conner et al., 2011; Crone et al., 1998; Edwards et al., 2005; Logothetis et al., 2001; Miller et al., 2007a; Miller et al., 2007b; Ray et al., 2008; Scheeringa et al., 2011). This provides complementary evidence to the fMRI findings in Experiment 1 of preSMA and rIFG activity for preparing to stop. However, it goes further by providing information about the relative timing of engagement of these regions. The significance of preSMA activity preceding rIFG when preparing to stop will be discussed below in relation to theories of action control.

**Outright Stopping: preSMA and rIFG:** While the high gamma band frequency points to neural activity within a region, lower frequencies may be important for long-distance communication between regions (Fries, 2005; van Elswijk et al., 2010; Womelsdorf et al., 2007). Prior research has implicated the beta band (13–30 Hz) as a candidate for communication in a putative prefrontal cortex/basal-ganglia network for action control (Kühn et al., 2004; Swann et al., 2011; Swann et al., 2009). Our earlier ECoG study specifically reported increases in the beta band in the rIFG when responses were stopped (Swann et al., 2009). Here we aimed to (1) replicate this finding in a new patient (and with a new task), (2) examine if beta amplitude also increases in the preSMA when stopping occurs and (3) determine if there is coherence between the rIFG and the preSMA during stopping in the beta band. Because we had this specific a-priori hypothesis, based on these previous studies, we did not apply a FDR correction for these results.

Time-locked to the stop signal, beta amplitude increases (~16 Hz) were indeed observed in both preSMA and rIFG beginning shortly after the stop signal (each region $p<0.01$, uncorrected, see Figure 5), compared to a pre-stimulus baseline (−500 to 0 ms relative to the stop signal). The beta response in rIFG was greater for MS_SS compared to MS_US trials ($p<0.05$, uncorrected, see Figure 5). Although this is similar to prior results (Swann et al., 2009) it is a more subtle effect, perhaps because of the increased expectation of stopping in this paradigm relative to the standard stopping paradigm (here p(stop|MS cue) was 50%, whereas p(stop) in the standard paradigm is usually ~25–33%). Unlike the rIFG, the

comparison of MS_SS vs. MS_US was not significant for the preSMA. Also evident in Figure 5 are differences in other frequency bands implicated in cognitive control, such as theta (Cavanagh et al., 2009; Luu et al., 2004; Marco-Pallares et al., 2008; Trujillo and Allen, 2007). Such findings are candidates for future exploration, however, because this was a relatively weak effect for which we did not have an a-priori hypothesis, we do not discuss it further here.

Thus, the response in the rIFG replicates our earlier results (Swann et al., 2009), and also shows a similar increase in beta band activity for the preSMA following the stop signal (and before SSRT), though there was not a significant difference for successful and unsuccessful stop trials for this region. [Note that there were also high gamma amplitude increases for outright stopping for both regions – these results are shown in the section below].

We examined task-related coherence between the preSMA and rIFG for MS_SS and MS_US trials. There was a significant increase in coherence in the beta band after the stop signal, but before SSRT elapsed, for MS_SS trials ($p<0.01$, uncorrected, see Figure 5), but not for MS_US trials. The difference in coherence between MS_SS and MS_US trials in the beta band was also significant ($p<0.01$, uncorrected, see Figure 5). Examination of phase lag can theoretically inform the directionality of the interaction, but in this case, the phase delay was near zero, suggesting overall network synchrony or that both regions may be driven by a third, unmeasured, region(s) (potentially the subthalamic nucleus) (Swann et al., 2011).

Taken together, these observations provide further evidence that the preSMA and the rIFG make up a structurally and physiologically connected circuit that is engaged in a task-related fashion.

**Outright Stopping: the wider cortical network:** To provide a fuller picture of the relative timing of preSMA and the rIFG, as well as other regions of putative interest for stopping such as the temporo-parietal junction (Corbetta and Shulman, 2002), the superior parietal region (Corbetta and Shulman, 2002), the auditory cortex, the middle frontal gyrus, and M1 (Swann et al., 2009) we examined high gamma activity for all electrodes in the right lateral cortex and the dorsomedial region. We focused on the period of 150 ms before the stop signal to 250 ms after it. Average high gamma (100 Hz) amplitude expressed as a z-score was calculated for MS_SS trials compared to baseline (the inter-trial interval) for each 50 ms time window. Significant responses ($p<0.01$, FDR corrected) are shown in Figure 6.

The middle frontal gyrus showed sustained activity across the trial. This could reflect working memory for the stopping rule (Goldman-Rakic, 1990; Muller and Knight, 2006; Olesen et al., 2004; Petrides, 2000). The intra-parietal sulcus/superior parietal lobe was active *early* in the trial, prior to stop signal onset, perhaps related to a putative role in top-down attention (Corbetta and Shulman, 2002)(See Supplementary Figure 8 for more detail and examination of this region during preparing to stop). In the more ventral region of the temporo-parietal junction there was, by contrast, activity following the stop signal, in line with its hypothesized role in bottom-up driven attention (Corbetta and Shulman, 2002) (See Supplementary Figure 9 for more detail and examination of this region during preparing to stop). Finally, both the (right) primary motor and primary auditory areas were active as would be expected with a task involving left hand responses and an auditory stop signal.

This analysis provides a map of the disseminated components of the stopping network and also complements the earlier results with the preSMA and rIFG (see Figure 5). The preSMA was significantly active as far back as 150 to 100 ms *before* the stop signal, with very strong activation occurring 50 to 0 ms prior to the stop signal and maintained past the estimated point at which SSRT elapses. By contrast, the rIFG was weakly active 100 to 50 ms before

the stop signal, but did not become strongly active until about 50 to 100 ms *after* the stop signal, peaking between 100 and 150 ms, and then maintaining activation past the estimated SSRT.

## DISCUSSION

We aimed to clarify the roles of the preSMA and the rIFG in action control. We designed a novel prepare-to-stop and outright-stop task, validated it with fMRI in healthy controls, and then examined ECoG during this task for a single rare patient with subdural coverage of the preSMA and rIFG. In healthy young controls fMRI showed that both the preSMA and the rIFG were more active for MS_Go compared to NS_Go trials – i.e. in preparation for stopping. By contrast, the rIFG alone was significantly active when comparing MS_SS and MS_Go trials – i.e. for outright stopping. We used the same behavioral paradigm in a single rare patient with intracranial grid coverage of both regions. In addition to task-related ECoG this patient was evaluated using several other methods. First, macrostimulation in the dorsomedial grid showed that only stimulation of the preSMA induced motor arrest. This method pointed especially to preSMA contact IH11. Second, deterministic tractography revealed that contact IH11 in particular had a projection to the rIFG region, with the correspondence closest to electrode LF16/15. Third, low intensity stimulation combined with simultaneous recording from all contacts showed that stimulation at IH11/12 induced CCEPs within 30 ms in rIFG, with LF16 showing one of the strongest responses. Together these results point to a structurally and functionally connected circuit between the preSMA and rIFG, and they specifically identify IH11 and LF16 as electrodes of interest for task-related ECoG. Examining these electrodes for preparing to stop showed high gamma amplitude increases with preSMA's activity preceding that of rIFG. For outright stopping high gamma amplitude changes were again detected and again these changes occurred earlier for preSMA compared to rIFG. Furthermore, beta amplitude increases were also observed following the stop signal with greater coherence between the two regions when stopping was successful compared to when it was unsuccessful.

### Preparing to stop and stopping outright: implications for theories of action control

For preparing to stop the ECoG results were mainly consistent with the fMRI results in healthy controls. There was an increase in high gamma activity, the frequency most closely associated with the BOLD signal (Conner et al., 2011; Logothetis et al., 2001; Scheeringa et al., 2011), for MS_Go vs. NS_Go trials in both the preSMA and the rIFG. Importantly, for MS_Go trials the preSMA response occurred even before the Go stimulus while the rIFG response began only after the Go stimulus – thus the preSMA preceded the rIFG. This timing difference speaks to different possible roles for each of these regions during action control. Since the preSMA was active early on and temporally nonspecifically, we speculate that it translates the stopping rule into the action system, and prepares other nodes in the `network' to perform action control (Rushworth et al., 2004). Within this network the rIFG may implement the action control by `putting the brakes' on behavior (Jahfari et al., 2009). Such an account is in line with its observed activation around the response time. Thus rIFG may play an inhibitory control role in slowing down response emission on a MS trial, and stopping the response outright on stop trials, perhaps via connections with the STN (Kühn et al., 2004; Swann et al., 2011; Swann et al., 2009). This interpretation of relative roles for preSMA and IFG fits a recent TMS study of action control on switch trials (Neubert et al., 2010). While their task differs from our own, it likely contains an `outright stopping' component as the ongoing action is canceled in favor of an alternative one. The results showed that preSMA was engaged 125 ms after a switch signal while the rIFG was engaged at 175 ms. Further, disruption of preSMA with rTMS affected the functional connectivity between the rIFG and M1. These results, like our own, are consistent with the possibility

that the preSMA plays a general task-configuration role by mediating rIFG function in action control.

A contrasting account argues that the rIFG is important for attentional monitoring/detection (Hampshire et al., 2010; Sharp et al., 2010) while the preSMA implements inhibitory control (Duann et al., 2009; Mostofsky and Simmonds, 2008; Sharp et al., 2010). It is possible that the early preSMA engagement reflects `setting up the inhibitory control' (the gamma response) and that rIFG monitors for the stop signal (gamma response) and detects it (beta response) and then conveys this information to the preSMA (coherent beta activity) which implements inhibitory control (beta response). However, the timing of action control in Neubert et al (2010) speaks against this account, and we also note that TMS (Verbruggen et al., 2010) and fMRI studies (Boehler et al., 2010; Cai and Leung, 2011; Chikazoe et al., 2009a) suggest that the rIFG plays an inhibitory control role in addition to an attentional one. Indeed, the presence of beta amplitude increases around the time of stopping in both regions argues against an attentional orienting role alone for the rIFG.

The coincident beta activity and coherence in both regions also suggests a third possibility: that inhibitory control is not implemented by the rIFG or the preSMA, but, rather, by the network as a whole including the basal ganglia (Kühn et al., 2004; Swann et al., 2011; Swann et al., 2009). Recently we reported that experimentally-induced modulation of the basal ganglia (specifically the subthalamic nucleus) alters the cortical signature of stopping in the beta band (Swann et al., 2011). This suggests that the beta band is important for long-distance communication between frontal cortex and the basal ganglia when stopping is needed, a notion supported by other observations of cortical-basal ganglia phase relationships in the beta band (Fogelson et al., 2006; Sharott et al., 2005). The current results are compatible with this `wider network' view because there was coherent activity in the beta band for the preSMA and the rIFG, more so on successful stop trials, without clear phase-lag differences.

A fourth possibility, also related to the wider network account, is that stopping is implemented by the basal ganglia, perhaps specifically the subthalamic nucleus, and this drives strong synchronization of beta activity within an overall connected preSMA/IFG/STN network – i.e. the apparent coherence between the preSMA and rIFG may not reflect direct communication so much as the influence of a third (potentially subcortical) source. Clearly further research is required to tease apart these different theories of action control in relation to the different `nodes' in this network.

### The limitations of a single patient

As the ECoG study was based on a single, rare, patient (with both dorsomedial and right lateral coverage), we are mindful that it is important to replicate these findings using ECoG, MEG or other approaches and also to show that activity at the observed times is causally important for behavior (e.g. using disruptive techniques such as TMS). Nevertheless, the results in the patient show strong cross method consistency. There were tight relationships for the preSMA/rIFG network with macrostimulation, CCEP, DTI and ECoG – something that would difficult to establish in a group study without all these methodologies. They are also consistent with the fMRI study in the 16 healthy participants performing the same task. Taken together, the results provide further evidence for a structurally and functionally connected network between the preSMA and the rIFG. They also go further than extant reports in providing key information about the relative timing of preSMA and rIFG when preparing to stop, and also about the coherence between these regions when outright stopping is required.

### Summary and Conclusions

We show that macrostimulation of a particular locus in the preSMA induced motor arrest; that lower intensity stimulation at this locus led to evoked responses at a specific locus in the rIFG within 30 ms, and that both of these loci were connected by white matter. Further, we showed, in the same patient, that these nodes of the structural/functional network were also specifically engaged during task performance. The response at the preSMA preceded the rIFG when preparing to stop. This is consistent with the theory that that the preSMA plays a task-configuration function (e.g. to prepare the brain's network to stop) while the rIFG is important for monitoring for the environmental need to stop and/or implementing inhibitory control. When the stop signal occurred both the preSMA and the rIFG showed responses in the beta band – a good candidate for inter-regional communication, and there was strong coherence between these regions. We speculate that the different activity patterns in high frequency (gamma) vs. lower frequency (beta) could reflect differences in recruitment of individual regions and network properties, with higher frequencies being associated with local neural activity and lower ones with long distance communication (Crone et al., 1998; Edwards et al., 2005; Fries, 2005; Miller et al., 2007a; Miller et al., 2007b; Ray et al., 2008). These results for outright stopping suggest that either these two regions work together to achieve inhibitory control, or that inhibitory control is implemented via another node, such as the basal ganglia, with subsequent synchronization of the overall connected network. While the current results cannot clearly adjudicate between these different theories of action control, they provide novel information about the relative timing of recruitment of the preSMA and the rIFG and functional connectivity between them.

## Supplementary Material

Refer to Web version on PubMed Central for supplementary material.

## Acknowledgments

Funding is gratefully received from NIH grant DA026452 to A.R.A (PI) and N.T. (co-PI). N.S is supported by an NSF Graduate Student Fellowship and a NIH training grant via the Institute for Neural Computation at UCSD. NT is also supported by a Clinical and Translational Award KL2 RR0224149 from the National Center for Research Resources.

## REFERENCES

Akers D, Sherbondy A, Mackenzie R, Dougherty R, Wandell B. Exploring connectivity of the brain's white matter with dynamic queries. IEEE Trans Vis. Comput. Graph. 2005; 11:419–430. [PubMed: 16138552]

Aron AR. From reactive to proactive and selective control: developing a richer model for stopping inappropriate responses. Biol Psychiatry. 2010; 69:e55–68. [PubMed: 20932513]

Aron AR, Behrens TE, Smith S, Frank MJ, Poldrack RA. Triangulating a cognitive control network using diffusion-weighted magnetic resonance imaging (MRI) and functional MRI. J Neurosci. 2007; 27:3743–3752. [PubMed: 17409238]

Aron AR, Poldrack RA. Cortical and subcortical contributions to Stop signal response inhibition: role of the subthalamic nucleus. J Neurosci. 2006; 26:2424–2433. [PubMed: 16510720]

Beckmann CF, Jenkinson M, Smith SM. General multilevel linear modeling for group analysis in FMRI. Neuroimage. 2003; 20:1052–1063. [PubMed: 14568475]

Boehler CN, Appelbaum LG, Krebs RM, Hopf JM, Woldorff MG. Pinning down response inhibition in the brain--conjunction analyses of the Stop-signal task. Neuroimage. 2010; 52:1621–1632. [PubMed: 20452445]

Cai W, Leung HC. Cortical activity during manual response inhibition guided by color and orientation cues. Brain Res. 2009; 1261:20–28. [PubMed: 19401178]

Cai W, Leung HC. Rule-guided executive control of response inhibition: functional topography of the inferior frontal cortex. PLoS One. 2011; 6:e20840. [PubMed: 21673969]

Canolty R, Soltani M, Dalal S, Edwards E, Dronkers N, Nagarajan S, Kirsch H, Barbaro N, Knight RT. Spatiotemporal dynamics of word processing in the human brain. Front. Neurosci. 2007; 1

Cavanagh JF, Cohen MX, Allen JJ. Prelude to and resolution of an error: EEG phase synchrony reveals cognitive control dynamics during action monitoring. J Neurosci. 2009; 29:98–105. [PubMed: 19129388]

Chambers CD, Bellgrove MA, Stokes MG, Henderson TR, Garavan H, Robertson IH, Morris AP, Mattingley JB. Executive "brake failure" following deactivation of human frontal lobe. J Cogn Neurosci. 2006; 18:444–455. [PubMed: 16513008]

Chambers CD, Garavan H, Bellgrove MA. Insights into the neural basis of response inhibition from cognitive and clinical neuroscience. Neurosci Biobehav Rev. 2009

Chevrier AD, Noseworthy MD, Schachar R. Dissociation of response inhibition and performance monitoring in the stop signal task using event-related fMRI. Hum Brain Mapp. 2007; 28:1347–1358. [PubMed: 17274022]

Chikazoe J. Localizing performance of go/no-go tasks to prefrontal cortical subregions. Curr Opin Psychiatry. 2010

Chikazoe J, Jimura K, Asari T, Yamashita K, Morimoto H, Hirose S, Miyashita Y, Konishi S. Functional dissociation in right inferior frontal cortex during performance of go/no-go task. Cereb Cortex. 2009a; 19:146–152. [PubMed: 18445602]

Chikazoe J, Jimura K, Hirose S, Yamashita K.-i. Miyashita Y, Konishi S. Preparation to Inhibit a Response Complements Response Inhibition during Performance of a Stop-Signal Task. J Neurosci. 2009b; 29:15870–15877. [PubMed: 20016103]

Conner C, Ellmore TM, Pieters TA, Disano M, Tandon N. Variability of the Relationship between Electrophysiology and BOLD-fMRI across Cortical Regions in Humans. Journal of Neuroscience. 2011 in press.

Corbetta M, Shulman GL. Control of goal-directed and stimulus-driven attention in the brain. Nat Rev Neurosci. 2002; 3:201–215. [PubMed: 11994752]

Crone NE, Miglioretti DL, Gordon B, Lesser RP. Functional mapping of human sensorimotor cortex with electrocorticographic spectral analysis. II. Event-related synchronization in the gamma band. Brain. 1998; 121(Pt 12):2301–2315. [PubMed: 9874481]

Dale AM, Fischl B, Sereno MI. Cortical surface-based analysis. I. Segmentation and surface reconstruction. Neuroimage. 1999; 9:179–194. [PubMed: 9931268]

Duann JR, Ide JS, Luo X, Li CS. Functional connectivity delineates distinct roles of the inferior frontal cortex and presupplementary motor area in stop signal inhibition. J Neurosci. 2009; 29:10171–10179. [PubMed: 19675251]

Edwards E, Soltani M, Deouell LY, Berger MS, Knight RT. High gamma activity in response to deviant auditory stimuli recorded directly from human cortex. J Neurophysiol. 2005; 94:4269–4280. [PubMed: 16093343]

Fogelson N, Williams D, Tijssen M, van Bruggen G, Speelman H, Brown P. Different functional loops between cerebral cortex and the subthalmic area in Parkinson's disease. Cereb Cortex. 2006; 16:64–75. [PubMed: 15829734]

Ford A, McGregor KM, Case K, Crosson B, White KD. Structural connectivity of Broca's area and medial frontal cortex. Neuroimage. 2010; 52:1230–1237. [PubMed: 20488246]

Forstmann BU, Anwander A, Schafer A, Neumann J, Brown S, Wagenmakers EJ, Bogacz R, Turner R. Cortico-striatal connections predict control over speed and accuracy in perceptual decision making. Proc Natl Acad Sci U S A. 2010; 107:15916–15920. [PubMed: 20733082]

Fried I, Katz A, McCarthy G, Sass KJ, Williamson P, Spencer SS, Spencer DD. Functional organization of human supplementary motor cortex studied by electrical stimulation. J Neurosci. 1991; 11:3656–3666. [PubMed: 1941101]

Fries P. A mechanism for cognitive dynamics: neuronal communication through neuronal coherence. Trends in Cognitive Sciences. 2005; 9:474–480. [PubMed: 16150631]

Garavan H, Ross TJ, Stein EA. Right hemispheric dominance of inhibitory control: an event-related functional MRI study. Proc Natl Acad Sci U S A. 1999; 96:8301–8306. [PubMed: 10393989]

Goldman-Rakic PS. Cellular and circuit basis of working memory in prefrontal cortex of nonhuman primates. Prog Brain Res. 1990; 85:325–335. discussion 335–326. [PubMed: 2094903]

Hampshire A, Chamberlain SR, Monti MM, Duncan J, OWEN AM. The role of the right inferior frontal gyrus: inhibition and attentional control. Neuroimage. 2010

Jahfari S, Stinear CM, Claffey M, Verbruggen F, Aron AR. Responding with Restraint: What Are the Neurocognitive Mechanisms? J Cogn Neurosci. 2009

Johansen-Berg H, Behrens TE, Robson MD, Drobnjak I, Rushworth MF, Brady JM, Smith SM, Higham DJ, Matthews PM. Changes in connectivity profiles define functionally distinct regions in human medial frontal cortex. Proc Natl Acad Sci U S A. 2004; 101:13335–13340. [PubMed: 15340158]

Kenner NM, Mumford JA, Hommer RE, Skup M, Leibenluft E, Poldrack RA. Inhibitory motor control in response stopping and response switching. J Neurosci. 2010; 30:8512–8518. [PubMed: 20573898]

Khursheed F, Tandon N, Tertel K, Pieters TA, Disano MA, Ellmore TM. Frequency-specific electrocorticographic correlates of working memory delay period fMRI activity. Neuroimage. 2011; 56:1773–1782. [PubMed: 21356314]

Konishi S, Nakajima K, Uchida I, Kameyama M, Nakahara K, Sekihara K, Miyashita Y. Transient activation of inferior prefrontal cortex during cognitive set shifting. Nat Neurosci. 1998; 1:80–84. [PubMed: 10195114]

Kühn AA, Williams D, Kupsch A, Limousin P, Hariz M, Schneider G-H, Yarrow K, Brown P. Event-related beta desynchronization in human subthalamic nucleus correlates with motor performance. Brain. 2004; 127:735–746. [PubMed: 14960502]

Leung HC, Cai W. Common and differential ventrolateral prefrontal activity during inhibition of hand and eye movements. J Neurosci. 2007; 27:9893–9900. [PubMed: 17855604]

Levy BJ, Wagner AD. Cognitive control and right ventrolateral prefrontal cortex: reflexive reorienting, motor inhibition, and action updating. Ann N Y Acad Sci. 2011; 1224:40–62. [PubMed: 21486295]

Logothetis NK, Pauls J, Augath M, Trinath T, Oeltermann A. Neurophysiological investigation of the basis of the fMRI signal. Nature. 2001; 412:150–157. [PubMed: 11449264]

Luders H, Lesser RP, Dinner DS, Morris HH, Wyllie E, Godoy J. Localization of cortical function: new information from extraoperative monitoring of patients with epilepsy. Epilepsia. 1988; 29(Suppl 2):S56–65. [PubMed: 3168959]

Luu P, Tucker DM, Makeig S. Frontal midline theta and the error-related negativity: neurophysiological mechanisms of action regulation. Clin Neurophysiol. 2004; 115:1821–1835. [PubMed: 15261861]

Marco-Pallares J, Camara E, Munte TF, Rodriguez-Fornells A. Neural mechanisms underlying adaptive actions after slips. J Cogn Neurosci. 2008; 20:1595–1610. [PubMed: 18345985]

Matsumoto R, Nair DR, LaPresto E, Bingaman W, Shibasaki H, Luders HO. Functional connectivity in human cortical motor system: a cortico-cortical evoked potential study. Brain. 2007; 130:181–197. [PubMed: 17046857]

Matsumoto R, Nair DR, LaPresto E, Najm I, Bingaman W, Shibasaki H, Luders HO. Functional connectivity in the human language system: a cortico-cortical evoked potential study. Brain. 2004; 127:2316–2330. [PubMed: 15269116]

Miller KJ, denNijs M, Shenoy P, Miller JW, Rao RPN, Ojemann JG. Real-time functional brain mapping using electrocorticography. Neuroimage. 2007a; 37:504–507. [PubMed: 17604183]

Miller KJ, Leuthardt EC, Schalk G, Rao RPN, Anderson NR, Moran DW, Miller JW, Ojemann JG. Spectral changes in cortical surface potentials during motor movement. J Neurosci. 2007b; 27:2424–2432. [PubMed: 17329441]

Mostofsky SH, Simmonds DJ. Response Inhibition and Response Selection: Two Sides of the Same Coin. J Cogn Neurosci. 2008

Muller NG, Knight RT. The functional neuroanatomy of working memory: Contributions of human brain lesion studies. Neuroscience. 2006:51–58. [PubMed: 16352402]

Nachev P, Kennard C, Husain M. Functional role of the supplementary and pre-supplementary motor areas. Nat Rev Neurosci. 2008; 9:856–869. [PubMed: 18843271]

Neubert FX, Mars RB, Buch ER, Olivier E, Rushworth MF. Cortical and subcortical interactions during action reprogramming and their related white matter pathways. Proc Natl Acad Sci U S A. 2010; 107:13240–13245. [PubMed: 20622155]

Olesen PJ, Westerberg H, Klingberg T. Increased prefrontal and parietal activity after training of working memory. Nat Neurosci. 2004; 7:75–79. [PubMed: 14699419]

Petrides M. The role of the mid-dorsolateral prefrontal cortex in working memory. Exp Brain Res. 2000; 133:44–54. [PubMed: 10933209]

Picard N, Strick PL. Activation of the supplementary motor area (SMA) during performance of visually guided movements. Cereb Cortex. 2003; 13:977–986. [PubMed: 12902397]

Ray S, Crone NE, Niebur E, Franaszczuk PJ, Hsiao SS. Neural correlates of high-gamma oscillations (60–200 Hz) in macaque local field potentials and their potential implications in electrocorticography. J Neurosci. 2008; 28:11526–11536. [PubMed: 18987189]

Rubia K, Smith AB, Brammer MJ, Taylor E. Right inferior prefrontal cortex mediates response inhibition while mesial prefrontal cortex is responsible for error detection. Neuroimage. 2003; 20:351–358. [PubMed: 14527595]

Rushworth MF, Walton ME, Kennerley SW, Bannerman DM. Action sets and decisions in the medial frontal cortex. Trends Cogn Sci. 2004; 8:410–417. [PubMed: 15350242]

Saad ZS, Ropella KM, DeYoe EA, Bandettini PA. The spatial extent of the BOLD response. Neuroimage. 2003; 19:132–144. [PubMed: 12781733]

Scheeringa R, Fries P, Petersson KM, Oostenveld R, Grothe I, Norris DG, Hagoort P, Bastiaansen MC. Neuronal dynamics underlying high- and low-frequency EEG oscillations contribute independently to the human BOLD signal. Neuron. 2011; 69:572–583. [PubMed: 21315266]

Sharott A, Magill PJ, Bolam JP, Brown P. Directional analysis of coherent oscillatory field potentials in the cerebral cortex and basal ganglia of the rat. The Journal of Physiology. 2005; 562:951–963. [PubMed: 15550466]

Sharp DJ, Bonnelle V, De Boissezon X, Beckmann CF, James SG, Patel MC, Mehta MA. Distinct frontal systems for response inhibition, attentional capture, and error processing. Proceedings of the National Academy of Sciences. 2010:1–6.

Sherbondy A, Akers D, Mackenzie R, Dougherty R, Wandell B. Exploring connectivity of the brain's white matter with dynamic queries. IEEE Trans Vis Comput Graph. 2005; 11:419–430. [PubMed: 16138552]

Swann N, Poizner H, Houser M, Gould S, Greenhouse I, Cai W, Strunk J, George J, Aron AR. Deep brain stimulation of the subthalamic nucleus alters the cortical profile of response inhibition in the beta frequency band: a scalp EEG study in Parkinson's disease. J Neurosci. 2011; 31:5721–5729. [PubMed: 21490213]

Swann N, Tandon N, Canolty R, Ellmore TM, McEvoy LK, Dreyer S, DiSano M, Aron AR. Intracranial EEG reveals a time- and frequency-specific role for the right inferior frontal gyrus and primary motor cortex in stopping initiated responses. J Neurosci. 2009; 29:12675–12685. [PubMed: 19812342]

Tandon, N. Cortical Mapping by Electrical Stimulation of Subdural Electrodes: Language areas. In: Luders, HO., editor. Textbook of Epilepsy Surgery. Informa HealthCare; New York: 2008. p. 1001-1015.

Tertel K, Tandon N, Ellmore TM. Probing brain connectivity by combined analysis of diffusion MRI tractography and electrocorticography. Comput Biol Med. 2010

Trujillo LT, Allen JJ. Theta EEG dynamics of the error-related negativity. Clin Neurophysiol. 2007; 118:645–668. [PubMed: 17223380]

van Elswijk G, Maij F, Schoffelen J-M, Overeem S, Stegeman DF, Fries P. Corticospinal beta-band synchronization entails rhythmic gain modulation. J Neurosci. 2010; 30:4481–4488. [PubMed: 20335484]

Verbruggen F, Aron AR, Stevens MA, Chambers CD. Theta burst stimulation dissociates attention and action updating in human inferior frontal cortex. Proc Natl Acad Sci U S A. 2010; 107:13966–13971. [PubMed: 20631303]

Vink M, Kahn RS, Raemaekers M, van den Heuvel M, Boersma M, Ramsey NF. Function of striatum beyond inhibition and execution of motor responses. Hum Brain Mapp. 2005; 25:336–344. [PubMed: 15852388]

Womelsdorf T, Schoffelen JM, Oostenveld R, Singer W, Desimone R, Engel AK, Fries P. Modulation of neuronal interactions through neuronal synchronization. Science. 2007; 316:1609–1612. [PubMed: 17569862]

Woolrich M. Robust group analysis using outlier inference. Neuroimage. 2008; 41:286–301. [PubMed: 18407525]

Woolrich MW, Behrens TE, Beckmann CF, Jenkinson M, Smith SM. Multilevel linear modelling for FMRI group analysis using Bayesian inference. Neuroimage. 2004; 21:1732–1747. [PubMed: 15050594]

Xue G, Aron AR, Poldrack RA. Common neural substrates for inhibition of spoken and manual responses. Cereb Cortex. 2008; 18:1923–1932. [PubMed: 18245044]

Zandbelt BB, Vink M. On the role of the striatum in response inhibition. PLoS One. 2010; 5:e13848. [PubMed: 21079814]

**Highlights**

- We used fMRI in healthy adults and multiple methods in a single epilepsy patient.
- We studied the presupplementary motor area and right inferior frontal gyrus.
- The preSMA and rIFG are structurally and functionally connected.
- Gamma activity in preSMA occurs before rIFG in anticipation of action control.
- Beta-band coherence between preSMA and rIFG occurs during action control.

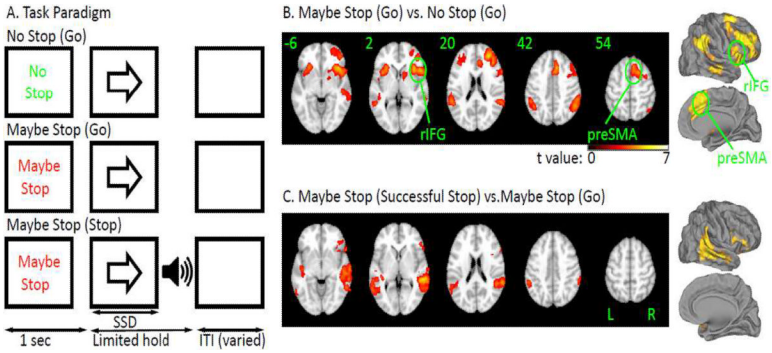


**Figure 1.**

A. Task. Each trial began with a cue (“Maybe Stop” or “No Stop”). Then, a left or right arrow (go signal) followed. Participants were instructed to quickly respond. On half the “Maybe Stop” trials, a beep (stop signal) was presented shortly after the go signal. Participants were instructed to try to inhibit their response when the beep was presented. B. Brain activation for preparing to stop. The contrast is MS_Go vs. NS_Go ($z>2.3$, $p<0.05$ cluster corrected); C. Brain activation for outright stopping. The contrast is MS_SS vs. MS_Go ($z>2.3$, $p<0.05$ cluster corrected).

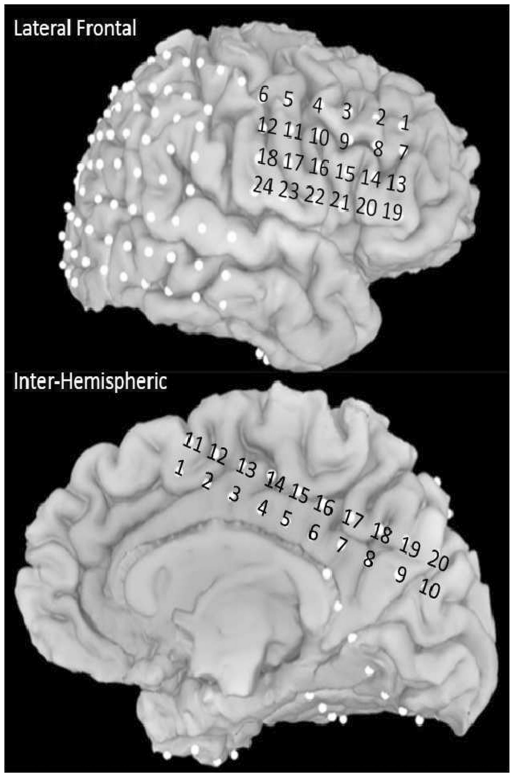


**Figure 2.**
Electrode locations for all electrodes in the preSMA and rIFG regions. IH = interhemispheric, LF = lateral frontal.

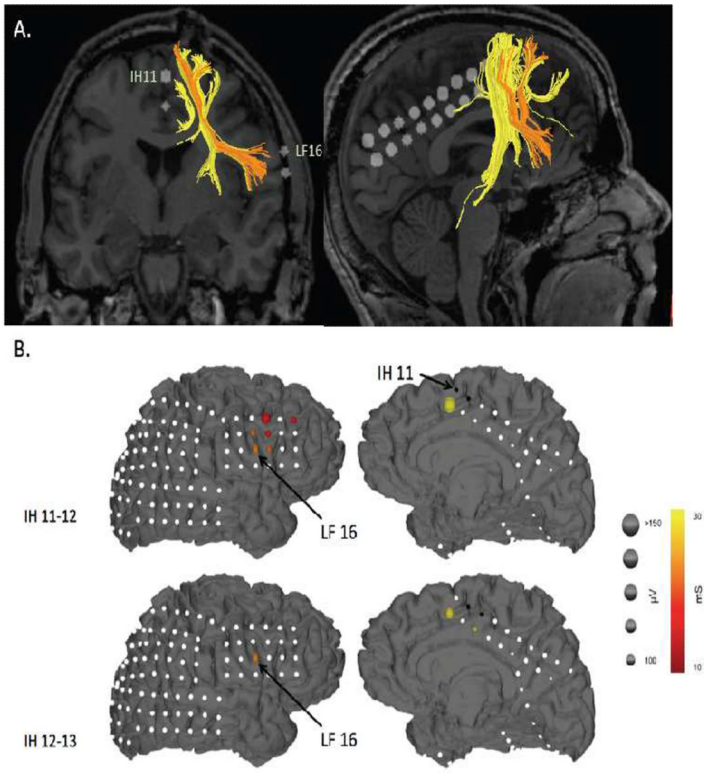


**Figure 3.**

A. Diffusion Tensor Imaging. Ipsilateral tracts between the preSMA and the right lateral frontal cortex are shown (only fibers with a mean FA value of greater than 4 and a length > 20 mm were displayed). Note that IH11 (preSMA) specifically connects to LF16 (rIFG). B. Cortico-cortical Evoked Potentials. Evoked potentials occurring within 30 ms following stimulation of the IH electrodes overlying pre-SMA. Responses to 50 epochs were averaged and are diagrammatically represented for each stimulating pair. Stimulating electrodes are black, electrodes with no CCEPs are white. CCEP magnitude (peak) is represented by the size and the time to peak of the CCEP is represented by the color of the spheroids placed at site of the electrodes. Distinct and spatially specific responses were noted in rIFG and MFG with pre-SMA stimulation.

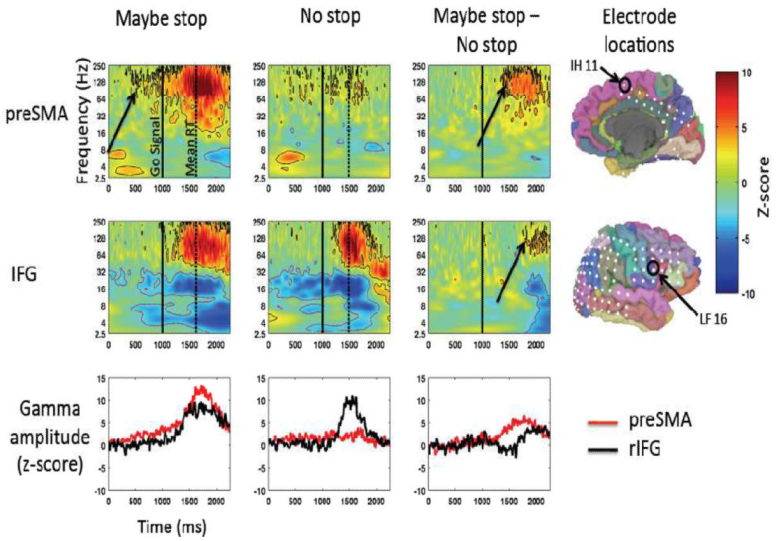


**Figure 4.**

ECoG: Preparing to stop for preSMA and rIFG. Gamma amplitude increases in preSMA precede those in rIFG. Zero ms is the time of the MS/NS cue and 1000 ms is the time of the go signal (indicated by the solid black line). The dotted line indicates mean RT. Z-scored amplitude is expressed in color. All results significant at $p<0.05$, FDR corrected are outlined (black indicates significance in positive direction, red indicates negative direction). Average amplitude for gamma (90–130 Hz) is shown plotted over time in the bottom row.

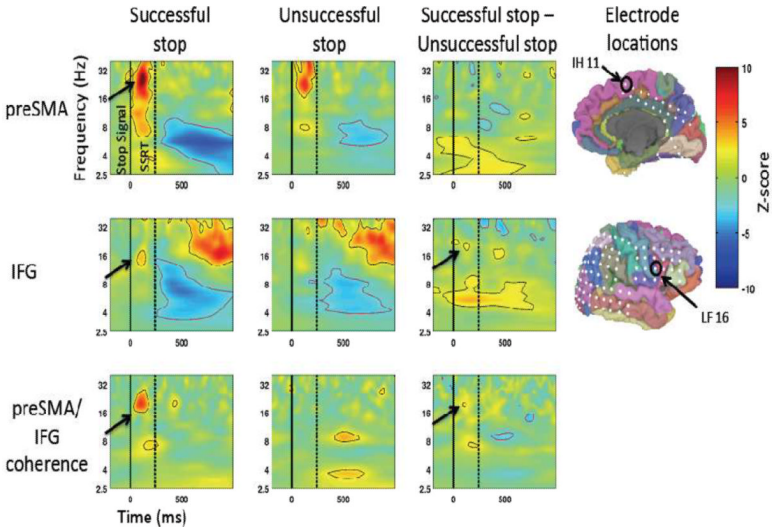


**Figure 5.**

ECoG: Outright stopping for preSMA and rIFG. There are beta amplitude increases in both regions following the stop signal. Additionally, coherence between the two is greater for successful compared to unsuccessful stopping. Zero ms is the time of the stop signal (indicated by the solid black line). The dotted line indicated SSRT. For the top 2 rows, Z-scored amplitude is expressed in color. All results that are significant ($p<0.01$, uncorrected, for the conditions relative to baseline and $p<0.05$ uncorrected for the difference) are outlined (black indicates significance in positive direction, red indicates negative direction). For the bottom row Z-scored coherence values are expressed in color. All results that are significant ($p<0.01$, uncorrected) are outlined (black indicates significance in positive direction, red indicates negative direction).

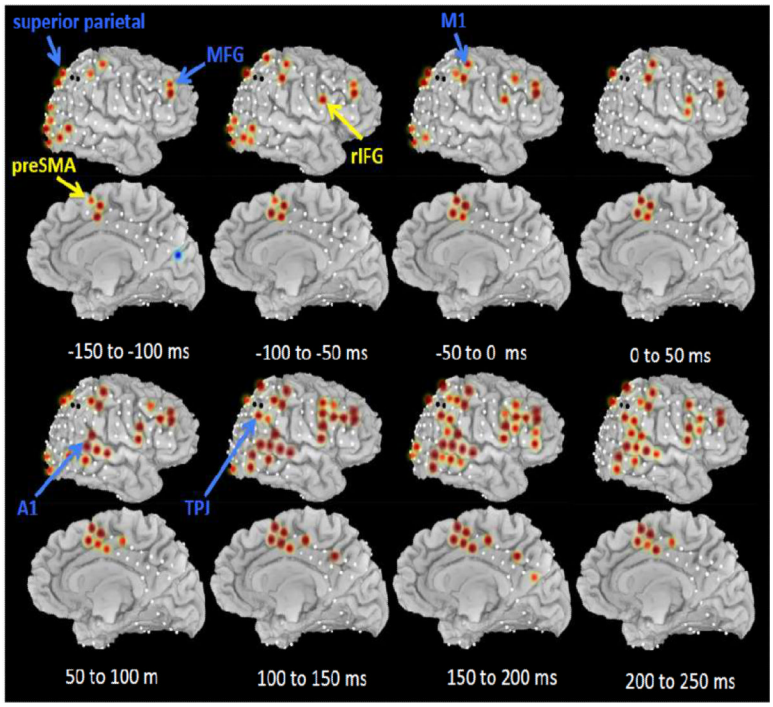


**Figure 6.**

ECoG: Outright stopping for the wider cortical network in the gamma band. Average high gamma (100 Hz) amplitudes (z-scored) are shown in color (red for increases relative to baseline, blue for decreases) for sequential 50 ms windows with 0 ms corresponding to the stop signal. Only values significant at $p<0.01$ FDR corrected are shown. Electrodes for which no data were available are indicated with a black circle.

## Table 1

Behavioral results.

| | Exp 1 fMRI: Mean (SD) | Exp 2 ECoG: Mean (SD) |
|---|---|---|
| NS_Go ACC (%) | 98.6 (1.8) | 94 (N/A) |
| NS_Go RT (ms) | 404 (42) | 491 (138) |
| MS_Go ACC (%) | 98.1 (3.6) | 93 (N/A) |
| MS_Go RT (ms) | 533 (91) | 618 (225) |
| MS_Stop ACC (%) | 69.9 (9.1) | 49 (N/A) |
| MS_Stop SSD (ms) | 281 (80) | 379 (84) |
| MS_Stop SSRT (ms) | 182 (50) | 239 (N/A) |

MS = Maybe Stop; NS = No Stop; ACC = Accuracy; SSD = stop signal delay; SSRT = Stop signal reaction time.

## Table 2

Macrostimulation results.

| Electrode Pairs | Current | Behavioral effects |
|---|---|---|
| **IH 1–2** | **3** | **Cessation of coordinated movement & articulation** |
| **IH 2–3** | **4** | **Cessation of coordinated movement & articulation** |
| IH 3–4 | 5 | Left leg flexion |
| IH 4–5, 5–6, 6–7, 7–8 | 10 | No change |
| IH 8–9, 9–10 | 8 | Visual hallucination: a pulsating phosphene in left inferior quadrant |
| **IH 11–12** | **8** | **Cessation of coordinated movement (bilaterally) & articulation** |
| IH 12–13 | 3 | Left leg flexion |
| IH 13–14 | 4 | Left arm and leg flexion and adduction |
| IH 14–15 | 4 | Left arm abduction |
| IH 15–16 | 4 | Left head versive movement, followed by whole body version |
| IH 16–17, 17–18, 18–19, 19–20 | 10 | No change |

The patient was tested at (i) rest (ii) while performing rapid hand closure and opening (such as making a signal for a flashing light) (iii) reading aloud and reciting the English alphabet. Channels shown in bold correspond to the anatomically defined preSMA. Current is in milliamperes, IH = interhemispheric electrodes (see Figure 2 for locations)